Multiple Feature Extraction for Content-Based Image Retrieval of Carotid Plaque Ultrasound Images

Christodoulos I. Christodoulou, Efthyvoulos Kyriacou, Costantinos S. Pattichis, Andrew Nicolaides

Abstract— **The extraction of multiple features from high-resolution ultrasound images of atherosclerotic carotid plaques characterizing the plaque morphology and structure can be used for the retrieval of similar plaques and the identification of individuals with asymptomatic carotid stenosis at risk of stroke. The objective of this work was to develop a computer aided system that will facilitate the automated retrieval of similar carotid plaque ultrasound images based on texture, shape, morphological, histogram and correlogram features, and the neural self organising map (SOM) and the statistical K-nearest neighbour (KNN) classifiers. The results in this work show that content-based image retrieval for carotid plaque image is feasible reaching a correct retrieval rate of 76%.**

I. Introduction

The huge amount of medical and other digital images made available in the recent days necessitate content-based image retrieval (CBIR) systems in order to effectively and efficiently use the information that is intrinsically stored in these image databases. A critical step for achieving this goal is the automated extraction of features characterizing the image. There was a lot of work in the last years for the construction of CBIR systems [1]. In [2] Laaksonen et al used the SOM classifier and different feature distributions for comparing different classes and different feature representations of the data in the context of the PicSOM CBIR system whereas Amores and Radeva [3] in their work presented a CBIR system for intravascular ultrasound images using a generalization of correlograms in order to extract local, global and contextual image features. In previous work [4] on the same problem with a different dataset, a highest correct retrieval rate of 73% was achieved.

The objective of this work was to develop a CBIR system that will facilitate the automated retrieval of similar carotid plaque ultrasound images based on the following features: (i) texture, (ii) shape, (iii) histogram,(iv) morphology and (v) correlogram. The aim was to identify plaque images with similar structure and based on their clinical history and known symptoms to decide the course of treatment for the test plaque/subject. The ultimate task was to identify individuals with asymptomatic carotid stenosis at risk of stroke [5]. Stroke is the third leading cause of death in the western world and the major cause of disability in adults.

C.I. Christodoulou, E. Kyriacou, and C.S. Pattichis are with the Department of Computer Science, University of Cyprus, Nicosia, Cyprus and with the Cyprus Institute of Neurology and Genetics, Nicosia, Cyprus; e-mail: {cschr2, ekyriac, pattichi}@ucy.ac.cy.

A. Nicolaides is with the Department of Vascular Surgery, Faculty of Medicine, Imperial College, University of London, UK.

II. Material

Ultrasound scans of carotid plaques were performed using duplex scanning and color flow imaging. A total of 336 carotid plaque ultrasound images (137 symptomatic and 199 asymptomatic) were analysed. For training the system 90 symptomatic and 90 asymptomatic plaques were used, whereas for evaluation of the system the remaining 109 symptomatic and 47 asymptomatic plaques were used. The carotid plaques were labeled as symptomatic after one of the following symptoms was identified: Stroke, transient ischemic attack or amaurosis fugax.

III. Feature Extraction

The following texture [6]-[11], shape, morphology [12], histogram and correlogram [2] feature sets were extracted from the segmented plaque images:

(a) Statistical Features (SF): The following statistical features were computed: 1) Mean value, 2) Median value, 3) Standard Deviation, 4) Skewness, and 5) Kurtosis.

(b) Spatial Gray Level Dependence Matrices (SGLDM): The spatial gray level dependence matrices as proposed by Haralick et al. [6] are based on the estimation of the second-order joint conditional probability density functions that two pixels (k,l) and (m,n) with distance d in direction specified by the angle θ, have intensities of gray level i and gray level j. Based on the probability density functions the following texture measures [6] were computed: 1) Angular second moment, 2) Contrast, 3) Correlation, 4) Sum of squares: variance, 5) Inverse difference moment, 6) Sum average, 7) Sum variance, 8) Sum entropy, 9) Entropy, 10) Difference variance, 11) Difference entropy, and 12), 13) Information measures of correlation. For a chosen distance d (in this work d=1 was used, i.e. 3x3 matrices) and for angles $\theta = 0^o$, 45^o, 90^o and 135^o we computed four values for each of the above 13 texture measures. In this work, the mean and the range of these four values were computed for each feature, and they were used as two different feature sets.

(c) Gray Level Difference Statistics (GLDS): The GLDS algorithm [7] uses first order statistics of local property values based on absolute differences between pairs of gray levels or of average gray levels in order to extract the following texture measures: 1) Homogeneity 2) Contrast, 3) Angular second moment, 4) Entropy, and 5) Mean. The above features were calculated for displacements $\delta = (0, d)$, (d, d), $(d, 0)$, $(d, -d)$, where $\delta \equiv (\Delta x, \Delta y)$, and their mean values were taken. In this work the parameter $d=1$ was used.

(d) Neighborhood Gray Tone Difference Matrix (NGTDM): Amadasun and King [8] proposed the Neighborhood Gray Tone Difference Matrix in order to extract textural features, which correspond to visual properties of texture. The following features were extracted, for a neighborhood size of (2d+1)x(2d+1) where $d=1$ was chosen: 1) Coarseness, 2) Contrast, 3) Busyness, 4) Complexity, and 5) Strength.

(e) Statistical Feature Matrix (SFM): The statistical feature matrix [9] measures the statistical properties of pixel pairs at several distances within an image, which are used for statistical analysis. Based on the SFM the following texture features were computed: 1) Coarseness, 2) Contrast, 3) Periodicity, and 4) Roughness. The constants L_r, L_c which determine the maximum intersample spacing distance were set L_r=L_c=4.

(f) Laws Texture Energy Measures (TEM): For the Laws TEM extraction [10], [11], vectors of length l=7, L=(1, 6, 15, 20, 15, 6, 1), E=(-1,-4,-5, 0, 5, 4, 1) and S=(-1,-2, 1, 4, 1,-2,-1) were used, where L performs local averaging, E acts as edge detector and S acts as spot detector. If we multiply the column vectors of length l by row vectors of the same length, we obtain Laws lxl masks. In order to extract texture features from an image, these masks are convoluted with the image and the statistics (e.g. energy) of the resulting image are used to describe texture. The following texture features were extracted: 1) LL - texture energy from LL kernel, 2) EE - texture energy from EE kernel, 3) SS - texture energy from SS kernel, 4) LE - average texture energy from LE and EL kernels, 5) ES - average texture energy from ES and SE kernels, and 6) LS - average texture energy from LS and SL kernels.

(g) Fractal Dimension Texture Analysis (FDTA): The Hurst coefficient $H^{(k)}$ [11] was computed for image resolutions k=1, 2, 3, 4. A smooth surface is described by a large value of the parameter H whereas the reverse applies for a rough surface.

(h) Fourier Power Spectrum (FPS): The radial sum and the angular sum of the discrete Fourier transform [11] were computed in order to describe texture.

(i) Shape: The following shape features were calculated from the plaque images [5]: 1) X - coordinate maximum length, 2) Y - coordinate maximum length, 3) Area, 4) Perimeter, and 5) Perimeter^2/Area. The idea was to investigate whether the size and complexity of the shape of the segmented plaque had any diagnostic value.

(j) Morphology: Morphological image processing allows the detection of the presence of specific patterns, called structural elements, at different scales. The simplest structural element for near-isotropic detection is the cross '+' consisting of five image pixels. Using the cross '+' as a structural element, pattern spectra were computed for each plague image as defined in [12]. The mean cumulative distribution functions (CDF) and the mean probability density functions (PDF) were computed as two different morphological feature sets.

(k) Histogram: The histogram of the plaque images was computed for 32 equal width bins and was used as an additional feature set. Histogram despite its simplicity provides a good description of the plaque structure.

(l) Correlogram: Correlograms are histograms which measure not only statistics about the features of the image, but also take into account the spatial distribution of these features [3]. In this work two correlograms were implemented: 1) based on the distance of the distribution of the pixels' gray level values from the center of the image, and 2) based on their angle of distribution. For each pixel the distance and the angle from the image center was calculated and for all pixels with the same distance or angle their histograms were computed. In order to make the comparison between images of different sizes feasible, the distance correlograms were normalized into 32 possible distances from the center by dividing the calculated distances with *maximum_distance/32*. The angle of the correlogram was allowed to vary among 32 possible values starting from the left middle of the image and moving clockwise. The resulting correlograms were matrices 32x253 (gray level values over 253 were set to be the white area surrounding the region of interest and were not consider for the calculation of the features).

The histogram and correlogram features were used for classification with their original values whereas the rest of the feature sets were normalized before use by subtracting their mean value and dividing with their standard deviation.

IV. Feature Selection

In order to enhance the classification yield, feature selection was implemented by computing the distance between the two classes for each feature as [5]:

$$dis = \frac{|m_1 - m_2|}{\sqrt{\sigma_1^2 + \sigma_2^2}} \quad (1)$$

where m_1 and m_2 are the mean values and σ_1 and σ_2 are the standard deviations of the two classes for each feature. The features with the highest discriminatory power were considered to be the ones with the greatest distance. The 15 best features were selected from the texture and morphology feature sets and were used as separate feature vectors. Furthermore, for the morphology features principal component analysis (PCA) was applied as another feature selection method.

V. Image Classification / Retrieval

For the retrieval of similar plaque images the neural self-organizing feature map (SOM) classifier and the statistical K-nearest neighbor (KNN) classifier were used:

(a) The SOM Classifier: The SOM was chosen because it is an unsupervised learning algorithm where the input patterns are freely distributed over the output node matrix [13]. The weights are adapted without supervision in such a way, so that the density distribution of the input data is preserved and represented on the output nodes. This mapping of similar input patterns to output nodes, which are close to each other, represents a discretisation of the input space, allowing a visualization of the distribution of the

input data. The output nodes are usually ordered in a two dimensional grid and at the end of the training phase, the output nodes are labeled with the class of the majority of the input patterns of the training set, assigned to each node.

In the evaluation phase, a new input pattern was assigned to the winning output node with the weight vector closest to the new input vector. In order to classify the new input pattern, the majority of the labels of the output nodes in an *RxR* neighborhood window centered at the winning node, were considered. The number of the input patterns in the neighborhood window for the two classes $m=\{1, 2\}$, (1=symptomatic, 2=asymptomatic), was computed as:

$$SN_m = \sum_{i=1}^{L} W_i N_{mi} \qquad (2)$$

where L is the number of the output nodes in the RxR neighborhood window with $L=R^2$ (e.g. $L=9$ using a 3x3 window), and N_{mi} is the number of the training patterns of the class m assigned to the output node i. $W_i=1/(2\ d_i)$, is a weighting factor based on the distance d_i of the output node i to the winning output node. W_i gives the output nodes near to the winning output node a greater weight than the ones farther away (e.g. in a 3x3 window, for the winning node W_i =1, for the four nodes perpendicular to the winning node W_i =0.5 and for the four nodes diagonally located W_i =0.3536, etc). The evaluation input pattern was classified to the class m of the SN_m with the greatest value, as symptomatic or asymptomatic.

(b) The KNN Classifier: The statistical k-nearest neighbor (KNN) classifier [14] was also used for the classification of the carotid plaques. In the KNN algorithm, in order to classify a new input pattern, its k nearest neighbors from the training set are identified. The new pattern is classified to the most frequent class among its neighbors based on a similarity measure that is usually the Euclidean distance. In this work the KNN carotid plaque classification system was implemented for different values of k and it was tested using for input the different feature sets.

For the SOM CBIR system, the retrieved images were assigned to the same output node with the test plaque or in the neighborhood window RxR of the winning node as explained above. In the KNN system the k most similar images using the Euclidean distance as the similarity measure were retrieved. The evaluation of how successful was the retrieval, was based on the classification of the retrieved plaques into two types: (i) symptomatic, or (ii) asymptomatic. If the type of the reference test plaque was the same with the type of the majority of the retrieved images, then the retrieval was considered successful.

VI. Results

Table I tabulates the success rates of correct retrievals for all cases for the SOM CBIR system, whereas Table II for the KNN system. In general the correlogram feature sets outperformed the rest in both systems, followed by the histogram and the texture feature sets. The morphology and the shape feature sets performed poorer in both systems.

More specific for the SOM system, best feature set in average was the correlogram (angle) with 72.0% correct retrievals, followed by the correlogram (distance) with 69.3%, the correlogram (both) with 68.6% when both correlograms were merged, and the histogram with 68.1%. Best texture feature set in average proved to be the GLDS with 66.4%, followed by the SF with 64.6% and the FDTA with 64.5%. The simple shape parameters performed worse with average correct retrievals 58.6% whereas morphology features also under- performed with highest rate being 58.8% when the best 15 features were selected from the PDF feature vector using Eq. 1. Using the PCA for feature selection on the morphology features did not improve the correct retrievals rate. Individually the highest rate was 75.6% for the correlogram (angle) and SOM window size 5x5.

Similarly for the KNN system, best feature set in average proved to be the correlogram (angle) with 74.3%, followed by the correlogram (both) with 74.1%, the correlogram (distance) with 69.7%, the histogram with 67.9% and the texture SGLDM (mean) and FDTA both with 65.0% correct retrievals. The highest correct retrieval rate for the morphology features was 60.8% when the best 15 features were selected from the CDF features using Eq. 1, whereas the shape parameters gave only 56.2%. Individually the highest rate was 76.3% for the correlogram (angle) and k=9.

Varying the values of k showed that bigger k values yielded in general better results as illustrated in the last row of Table II. This was true also for the SOM system for bigger window sizes, as shown in Table I. The SOM and the KNN classifiers performed exactly the same with overall average performance 61.9% for both classifiers.

In Figure 1 an example is given with the five more similar plaques to the reference plaque shown at the top left side of the figure. Below each plaque its label as symptomatic or asymptomatic is given. In Figure 1 the KNN classifier was used with the SGLDM (mean) texture feature set used as input. As seen from the labels of the retrieved images, 4 out 5 of the retrieved images are labeled as asymptomatic and their label coincides with the label of the reference plaque.

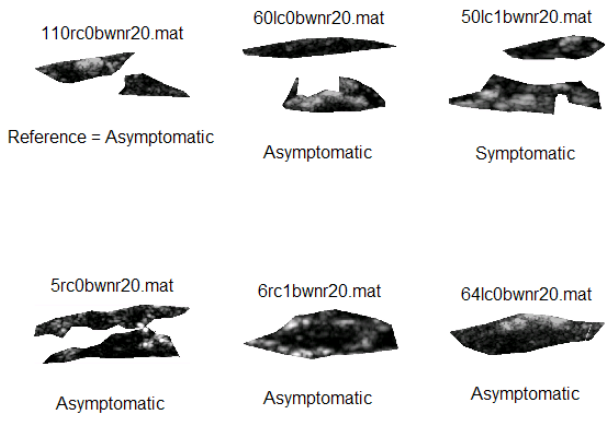

Fig. 1: Image retrieval using the KNN classifier and the texture feature set SGLDM (mean).

TABLE I

THE SUCCESS RATE OF CORRECT RETRIEVALS IN % FOR THE SOM CBIR SYSTEM, USING AS INPUT THE TEXTURE, THE SHAPE, THE MORPHOLOGY, THE HISTOGRAM, AND THE CORRELOGRAM FEATURE SETS. THE RESULTS ARE GIVEN FOR DIFFERENT SOM WINDOW SIZES AND IN AVERAGE. IN THE SECOND COLUMN *N* THE SIZE OF THE INPUT FEATURE VECTOR IS GIVEN. IN BOLD ARE HIGHLIGHTED THE BEST RESULTS PER FEATURE SET AND IN AVERAGE

Feature Set	*N*	*1x1*	*3x3*	*5x5*	*7x7*	*9x9*	*11x11*	*Average*
SF	5	62.0	64.1	63.0	66.5	64.7	**67.1**	***64.6***
SGLDM (mean)	13	60.7	61.3	62.6	63.9	64.3	**65.4**	*63.0*
SGLDM (range)	13	58.1	60.7	60.3	64.1	**64.3**	63.9	*61.9*
GLDS	4	63.5	66.0	66.2	67.3	**68.2**	67.3	***66.4***
NGTDM	5	61.1	62.0	62.8	63.9	65.2	**65.6**	*63.4*
SFM	4	59.2	60.3	60.9	**63.0**	61.1	61.1	*60.9*
TEM	6	52.4	54.3	56.2	**59.2**	58.8	58.8	*56.6*
FDTA	4	62.8	64.7	**65.2**	65.2	65.2	63.9	***64.5***
FP	2	58.1	58.8	61.1	**62.4**	61.3	61.5	*60.5*
All texture	56	62.0	62.8	66.0	64.7	**66.2**	63.7	*64.2*
Best 15 texture	15	59.0	63.0	65.2	66.0	**67.1**	66.9	***64.5***
Shape	5	55.3	57.7	59.4	59.8	58.8	**60.7**	*58.6*
Morphology CDF	57	49.1	50.0	51.9	53.8	56.6	**57.1**	*53.1*
Best 15 CDF	15	45.3	46.6	50.4	51.1	63.2	**66.7**	*53.9*
PCA CDF	5	53.6	**54.5**	50.6	50.0	53.6	53.0	*52.6*
Morphology PDF	57	54.9	57.7	57.3	59.8	60.3	**61.3**	*58.5*
Best 15 PDF	15	60.3	58.1	**60.5**	58.8	56.6	58.8	*58.8*
PCA PDF	11	**59.4**	55.8	55.8	56.8	56.8	57.7	*57.1*
Histogram	32	62.8	65.6	67.9	69.7	70.3	**72.0**	***68.1***
Correlogram (dist.)	32x253	62.2	66.0	69.9	72.4	72.4	**73.1**	***69.3***
Correlogram (angle)	32x253	61.5	75.0	**75.6**	75.0	73.1	71.8	***72.0***
Correlogram (both)	64x253	56.4	65.4	70.5	72.4	**74.4**	72.4	***68.6***
Average		*58.2*	*60.5*	*61.8*	*63.0*	*63.7*	*64.1*	*61.9*

TABLE II

THE SAME AS TABLE I FOR THE KNN CBIR SYSTEM AND DIFFERENT VALUES OF *K*

Feature Set	*N*	*k=1*	*k=3*	*k=5*	*k=7*	*k=9*	*k=11*	*k=37*	*Average*
SF	5	**63.5**	62.8	60.3	62.8	62.2	60.3	62.8	*62.1*
SGLDM (mean)	13	56.4	63.5	67.9	68.6	63.5	64.7	**70.5**	***65.0***
SGLDM (range)	13	56.4	62.8	65.4	64.7	**67.3**	63.5	66.7	*63.8*
GLDS	4	64.1	62.2	63.5	62.2	63.5	64.7	**69.2**	***64.2***
NGTDM	5	55.8	62.2	**64.1**	61.5	60.3	60.9	64.1	*61.3*
SFM	4	52.6	58.3	58.3	61.5	**62.2**	62.2	60.3	*59.3*
TEM	6	55.8	55.8	52.6	53.8	54.5	57.7	**58.3**	*55.5*
FDTA	4	55.1	66.0	65.4	66.0	**68.6**	67.3	66.7	***65.0***
FP	2	54.5	56.4	57.7	58.3	**62.2**	60.9	54.5	*57.8*
All texture	56	60.3	61.5	63.5	64.7	64.1	65.4	**66.7**	*63.7*
Best 15 texture	15	56.4	61.5	60.9	59.6	67.9	65.4	**70.5**	*63.2*
Shape	5	56.4	55.1	53.8	55.8	54.5	58.3	**59.6**	*56.2*
Morphology CDF	57	55.1	51.3	58.3	54.5	52.6	52.6	**63.4**	*55.4*
Best 15 CDF	15	58.3	53.8	57.1	60.3	61.5	**68.6**	66.0	*60.8*
PCA CDF	5	53.2	48.7	55.8	54.5	51.3	50.6	**60.2**	*53.5*
Morphology PDF	57	56.4	54.5	53.2	56.4	57.1	58.3	**64.1**	*57.1*
Best 15 PDF	15	54.5	55.1	57.7	59.6	**62.2**	57.7	50.6	*56.8*
PCA PDF	11	53.8	52.6	54.5	53.2	54.5	51.3	**62.8**	*54.7*
Histogram	32	64.7	63.5	65.4	69.2	70.5	66.7	**75.0**	***67.9***
Correlogram (dist.)	32x253	**72.4**	68.0	67.3	71.8	69.2	68.0	71.2	***69.7***
Correlogram (angle)	32x253	72.4	71.2	74.4	75.6	**76.3**	76.3	73.7	***74.3***
Correlogram (both)	64x253	72.4	71.2	74.4	75.0	**76.3**	76.3	73.1	***74.1***
Average		*59.1*	*59.9*	*61.4*	*62.3*	*62.8*	*62.6*	***65.0***	*61.9*

Figures 2, 3 and 4 show the retrieved images for the same reference plaque using the KNN with the FDTA, the histogram and the morphology feature sets respectively. Figures 5 and 6 illustrate the same example for the two correlogram feature sets. Figure 7 shows the correlogram (distance) and the correlogram (angle) for the reference image.

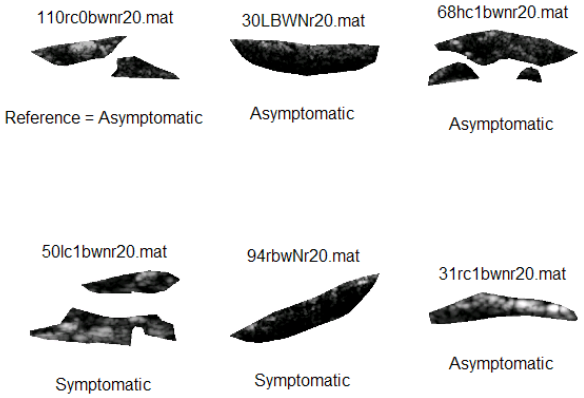

Fig. 2: Image retrieval using the KNN classifier and the texture feature set FDTA.

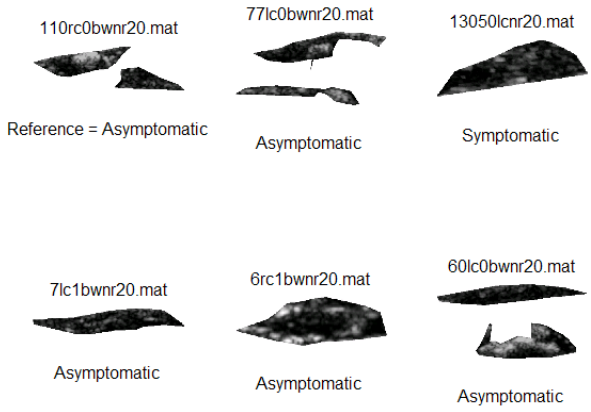

Fig. 3: Image retrieval using the KNN classifier and the histogram feature set.

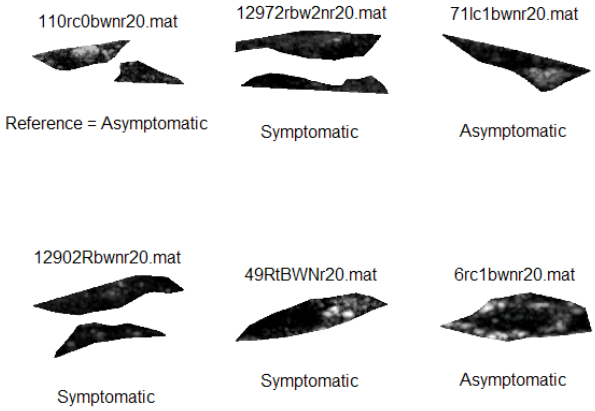

Fig. 4: Image retrieval using the KNN classifier and the morphology CDF feature set.

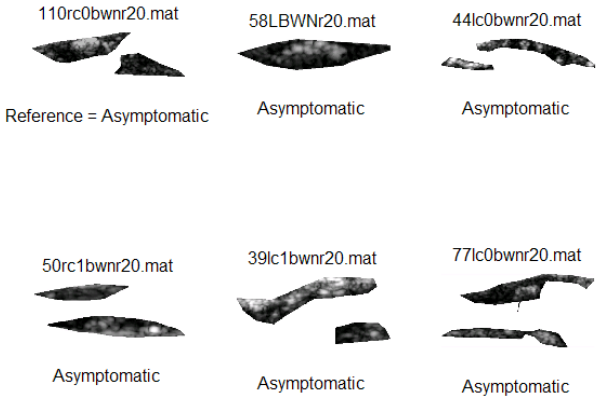

Fig. 5: Image retrieval using the KNN classifier and the correlogram (distance) feature set.

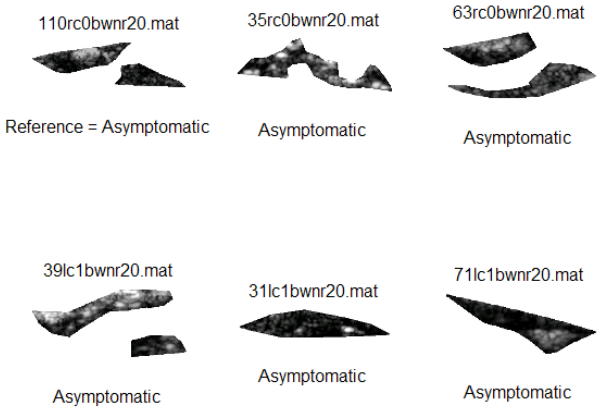

Fig. 6: Image retrieval using the KNN classifier and the correlogram (angle) feature set.

Fig. 7: The 32x253 matrices of the correlogram (distance) and below of the correlogram (angle) of the reference image 110rc0bwnr20.

VII. Conclusions

In this work an image retrieval system for carotid plaque ultrasound images is presented using as input multiple feature sets and based on the neural SOM and the statistical KNN classifiers. Best results were obtained when using the correlogram features, especially when the angle distribution was considered. This proves that the layout of the white calcified parts of the plaque in the ultrasound image, compared to the black soft parts of the image has a diagnostic value and affects whether a plaque will be symptomatic or asymptomatic.

The highest individual diagnostic yield was 76.3% for the correlogram (angle) with the KNN and k=9 and it was higher than previous work on the same problem

[4], [5]. Also the simple histogram feature performed quite well with highest retrieval rate 75.0% when the KNN was used with k=37. Traditional texture features like SGLDM (mean), GLDS, SF and FDTA also performed well as also demonstrated in previous work [4], [5], with highest retrieval rate being 70.5% for the SGLDM (mean) with the KNN and k=37. More complex features like morphology failed to perform up to the expectations for the specific problem.

The performance of the KNN and the SOM classifiers was similar. However the simpler statistical KNN classifier made it easier to track back and repeat the results than the more complex neural SOM classifier, which required separate training and evaluation phases. Also the SOM required optimization of the training process by selecting the correct network architecture and was computationally heavier especially in the case of the large feature vectors.

Future work will focus in combining the decisions made using the multiple feature sets into a single output through a combining weighting scheme. Furthermore the whole classification system will be incorporated in an automated CBIR system, which through a user-friendly interface will provide to the physician not only the labels of the retrieved plaques but also all the information about the original ultrasound images, the clinical data and the history of the similar cases. This will help the physician to decide the course of treatment and may spare patients from an unnecessary endarterectomy.

In conclusion the results in this work show that content-based image retrieval for carotid plaque images is feasible and that correlogram, histogram and texture features can be used successfully for the identification of cases with similar symptoms output.

ACKNOWLEDGMENT

This work was partly supported through the project *Integrated System for the Evaluation of Ultrasound Imaging of the Carotid Artery (TALOS)* of the Research Promotion Foundation of Cyprus.

REFERENCES

[1] Rui Y, Huang T.S., and Chang S., "Image retrieval: Current techniques, promising directions, and open issues," *J. Vis. Commun. Image Represent.*, vol. 10, no. 1,pp. 39-62, Mar. 1999.

[2] Laaksonen J., Koskela M., Oja E., "Class Distributions on SOM Surfaces for Feature Extraction and Object Retrieval", *IEEE Transactions on Neural Networks*, vol. 17(8-9), pp. 1121-1133, Oct.-Nov. 2004.

[3] Amores J, Radeva P., "Medical image retrieval based on plaque appearance and image registration" *Plaque Imaging: Pixel to Molecular Level, J.S. Suri (Eds.) IOS Press,* 2005.

[4] Christodoulou C.I., Pattichis C.S., Kyriacou E., Nicolaides A., "Content-Based Image Retrieval For Carotid Plaque Ultrasound Images", in *Proc. of EMBEC'05, 3rd European Medical and Biological Engineering Conference*, November 20- 25, 2005, Prague, Czech Republic.

[5] Christodoulou C.I., Pattichis C.S., Pantziaris M., Nicolaides A., "Texture Based Classification of Atherosclerotic Carotid Plaques", *IEEE Transactions on Medical Imaging*, vol. 22, pp. 902-912, July 2003.

[6] Haralick R.M., Shanmugam K., Dinstein I., "Texture Features for Image Classification", *IEEE Transactions on Systems, Man and Cybernetics,* Vol. SMC-3, pp. 610-621, Nov. 1973.

[7] Weszka J.S., Dyer C.R., Rosenfield A., "A Comparative Study of Texture Measures for Terrain Classification", *IEEE Transactions on Systems, Man and Cybernetics,* Vol. SMC-6, April 1976.

[8] Amadasun M., King. R., "Textural Features Corresponding to Textural Properties", *IEEE Transactions on Systems, Man and Cybernetics*, Vol. 19, No 5, pp.1264-1274, Sept./Oct. 1989.

[9] Wu Chung-Ming, Chen Yung-Chang, "Statistical Feature Matrix for Texture Analysis", *CVGIP: Graphical Models and Image Processing,* Vol. 54, No 5, pp. 407-419, Sept. 1992.

[10] Laws K.I., "Rapid Texture Identification", *SPIE, 1980,* Vol. 238, pp. 376-380.

[11] Wu Chung-Ming, Chen Yung-Chang, Hsieh Kai-Sheng, "Texture Features for Classification of Ultrasonic liver Images", *IEEE Transactions on Medical Imaging,* Vol. 11, No 2, pp. 141-152, June 1992.

[12] Dougherty E.R., *An Introduction to Morphological Image Processing*, Belingham, Washington, SPIE Optical Engineering Press, 1992.Kohonen T., "The Self-Organizing Map", *Proceedings of the IEEE*, Vol. 78, No. 9, pp. 1464-1480, Sept. 1990.

[13] Kohonen T., "The Self-Organizing Map", *Proceedings of the IEEE*, Vol. 78, No. 9, pp. 1464-1480, Sept. 1990.

[14] Tou J.T., Gonzalez R.C., *Pattern Recognition Principles*, Addison-Wesley Publishing Company, Inc., 1974.